Underwater vehicle speedometry using differential pressure sensors: Preliminary results

Juan F. Fuentes-Pérez[1,✉], Kaia Kalev[1], Jeffrey A. Tuhtan[1] and Maarja Kruusmaa[1]
[1]Centre for Biorobotics, Tallinn University of Technology, Tallinn, Estonia
[✉]E-mail: juan.fuentes@ttu.ee

***Abstract*— Underwater vehicles require accurate speedometry relative to local flow conditions to perform many tasks within the aquatic environment. This paper presents preliminary results of a differential pressure sensing system using an extension of the Pitot equation capable of providing instantaneous flow speed estimation, including yaw angles from ±45º. In contrast to systems with similar configuration based on absolute pressure sensor approaches, the differential system makes use of the pressure between two points on the sensor head, reducing the number of necessary sensors by half. The theoretical system performance and physical prototype are compared using computational fluid dynamics and flow tunnel tests from 0-0.5 m/s and angles of attack up to ±45º. The proposed speedometry device has a small form factor, uses inexpensive commodity hardware, is geometrically simple, accurate (mean absolute error of 0.024 m/s) and has low power consumption (< 10 mW for each sensor) making it suitable for a wide spectrum of underwater vehicles.**

Keywords*— speedometry, pressure sensors, lateral line, underwater robotics

I. Introduction

Accurate, real-time speed and flow measurements provide useful information for an autonomous underwater vehicle (AUV) to perform integral tasks such as localization or state estimation.

Conventional methods to estimate flow and speed in AUVs are based on acoustic Doppler current profilers (ADCPs) and Doppler velocity logs (DVLs) [1]. ADCPs can measure the global flow speed relative to the vehicle and, similarly, using the same working principle, the DVLs can provide an accurate measurement of AUVs speed relative to the seafloor [2]. Both devices are suitable tools to facilitate underwater navigation [1]–[3], but are expensive, bulky and have high energy consumption [4]. This renders acoustic methods unsuitable for some applications, especially small underwater vehicles which have strict payload size limitations [4], [5] or for prolonged missions with low energy requirements such as those performed by gliders [6]. Moreover, DVLs require a seafloor, or similar (e.g. sea ice), to provide a velocity measurement and ADCPs, do not measure local flows (i.e. flow around the vehicle) [4], which may introduce a source of error.

Recently, bioinspired flow sensing platforms based on fish' lateral lines have been proposed as an alternative for flow and speed estimation. Artificial lateral lines (ALLs) aim to mimic the flow sensing modalities present in fish by distributing a set of collocated sensing units over a robot or probe body. Similar to aquatic vertebrates, ALLs use the interaction between the body and surrounding flow field to detect and differentiate body-oriented changes in the flow field. Furthermore, bioinspired flow sensing platforms have overcome some limitations of previously mentioned methods. For example, they have the potential of measuring flows around the robot, are inexpensive and have low energy consumption [4], [5], [7], [8].

In addition to the bioinspired motivation, the relation between velocity and pressure is extensively known in aeronautics and hydraulics for flow speed estimation [9]. Moreover, Pitot tubes [10] and turbulence probes [11], [12] are devices that make use of pressure distribution over a flow-oriented body to estimate air speed and its fluctuations. Pitot devices have proven to be accurate and robust, finding widespread general use in aircraft navigation [10], [13] and for atmospheric monitoring [12], [14].

Taking into account the above, absolute pressure sensors have the potential of providing the robot's speed when navigating in still water conditions and can serve as a complement for the calculation of relative speed in moving water when the data is combined with a secondary estimate of craft speed or using an ancillary flow measuring device (e.g. ADCP or DVL). However, the static pressure component in water (depth) limits the application of this technology for the estimation of low speeds (< 0.15 m/s) [15]. This is due to two main reasons: (1) the relation between velocity and pressure is quadratic and thus high sensitivities are needed for low velocity estimations and (2) the static component of pressure causes the necessity of large pressure ranges, which is incompatible with high sensitivities.

In order to overcome these restrictions, we have developed a new differential pressure sensor (DPS) platform for flow speed estimation. DPS has several advantages over APS: (1) DPS devices measure the pressure difference across two points on the body, reducing the overall number of necessary sensors and (2) in contrast to APS, the static pressure component (i.e. depth component) is mechanically filtered in real-time, which increases the allowable sensor sensitivity providing a commensurate increase in the estimation accuracy.

Together with the developed DPS based system for achieving accurate real time flow speed estimations, we have proposed an extension of the commonly-applied Pitot equation [9], that allows the instant local flow speed estimation relative to the robot, independently of the angle of attack. We provide a new complement for underwater robotics with a simple design and signal processing method which is easy to construct and model, has low power consumption and high sampling rate to deliver real-time flow speed information.

II. Materials and Methods

The system performance and the final model were first studied by means of computational fluid dynamics (CFD) simulations. After an optimization of the body shape and the analysis of flow-body interaction, the prototype device was developed and physically tested in a flow tunnel.

A. Simulations

The CFD simulations were performed using the open source software *OpenFOAM* [16]. The model of the experimental platform (further described in II.B) was simplified to 2D domain and a laminar flow. Taking into account this, all cases were solved using the *pimpleFoam* solver, which is the built–in solver in *OpenFOAM* for large time-step transient incompressible flows, using the PIMPLE (merged PISO-SIMPLE) algorithm [17].

The standard configuration, with 0º angle of attack is shown in Fig. 1. A total of 24 scenarios were studied: 4 angles of attack (0º, 15º, 30º, 45º) and 6 flow speeds for each angle (0, 10, 20, 40, 50 cm/s).

B. Experimental Platform

A physical prototype (Fig. 2) was developed to validate the simulation results and to test the applicability of the proposed method. The prototype consists of a 3D printed "bullet" box. The design is simple and highly modular in order to study different possible configurations.

The system consists of two digital temperature compensated DPSs (SSCDRRN005ND2A5 [18]) of 0.15 Pa/LSB and a power consumption lower than 10 mW [18]. The digital signal is transmitted to a I2C multiplexer (TCA9548A [19]), which allows the control of each sensors with an

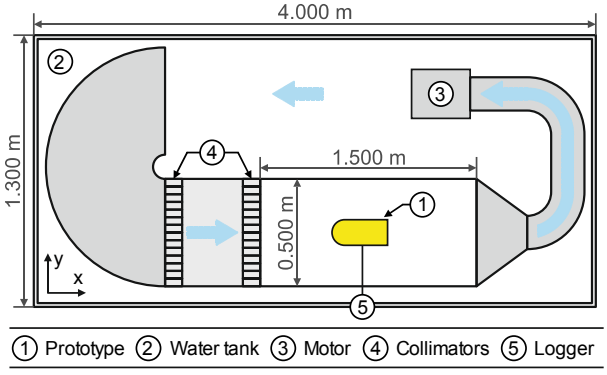

Figure 1. Top view of the experimental flume.

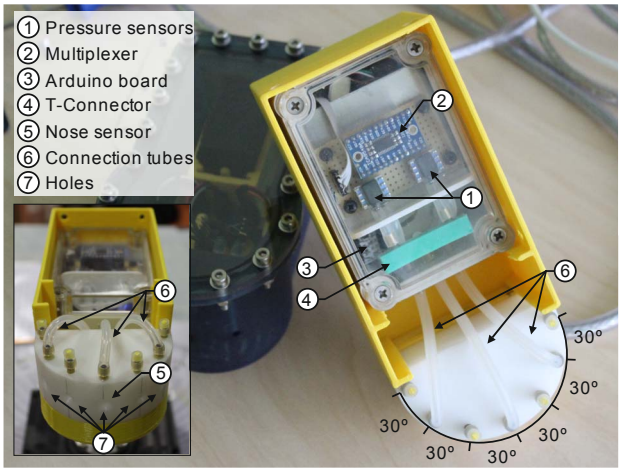

Figure 2. Physical platform used in the experiments. In the picture, top cover has been removed to show the internal components. The distribution of the tubes presented is the one used for this work.

Arduino micro board [20]. The sampling rate was fixed to 200 Hz for the conducted experiments.

Both sensors had two pressure ports. Each sensor's first port was connected to the nose (0º) via a T-connector (4 in Fig. 2), to record the stagnation point [9] when the angle of attack was equal to 0º (5 in Fig. 2). The second ports were connected at ±60º (one sensor on each side).

Several alternative connections were tested (6 in Fig. 2) using the array of flexible silicone tubes (1.6 mm bore size and wall thickness): 2 different orientations (horizontal and vertical), 3 different pressure sensors, 3 different port sizes (1, 2 and 3 mm of diameter) and 2 difference tube lengths (5 and 15 cm). The location, orientation and diameter of the ports in the head (7 in Fig. 2) were identified as the most influential factors for robust velocity estimation. Based on the results of the laboratory testing, it was concluded that (1) only one phase separation must exist in the tube and (2) constant offset due to the different quantities or air in the connections are better controlled with shorter tubes. The selected final configuration for the ports was a vertical orientation and 3 mm of diameter.

C. Experimental setup

Experiments were conducted in a flow tunnel with a closed working section of 0.5 m x 0.5 m x 1.5 m (see Fig. 1).

The flow in the tunnel was generated using an A/C motor and transmitted to the working section using a U-shaped flow strengthener and two sequential collimators. The water level in the flow tunnel was between 0.72-0.75 m during all the measurements.

The prototype was mounted in the middle of the working section facing the flow. For angle and flow speed measurements the prototype was rotated in the xy-plane while keeping the depth constant.

Two tests were performed for training and validation. In each test, 4 different angles (0º, 15º, 30º, 45º) were studied and 11 flow speeds were recorded for each angle over the range of 0-50 cm/s, with a step of 5 cm/s. Each measurement was

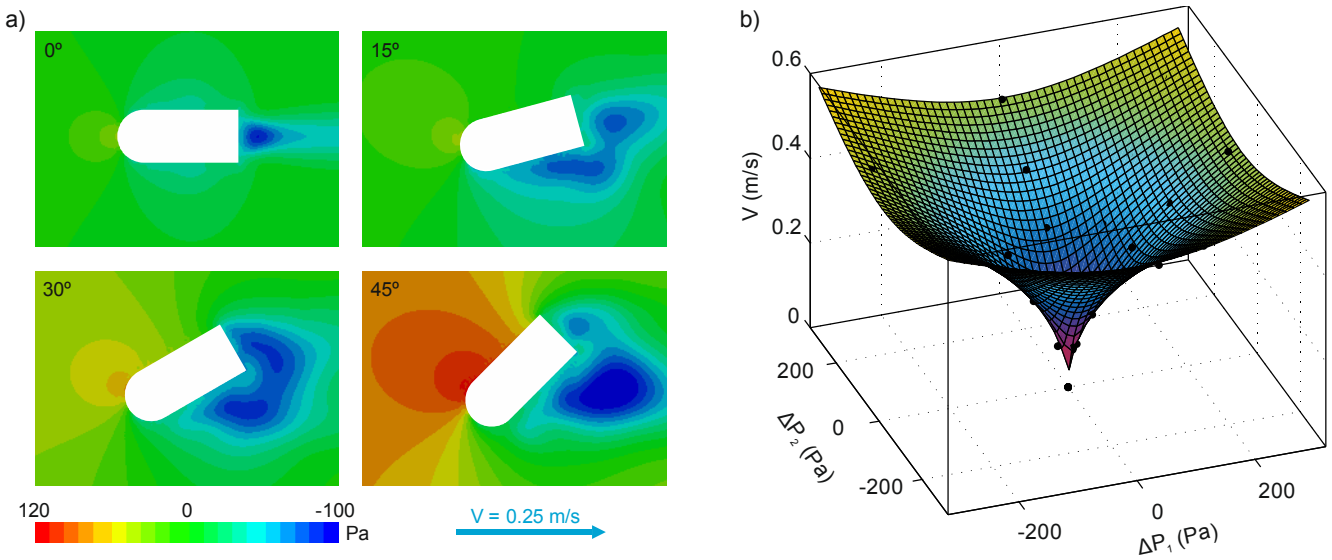

Figure 3. Summary of simulation results. a) Pressure distribution over the simulated model for different angles of attack and a velocity of 0.25 m/s. b) Fitted model considering all the simulated scenarios (port separation equal to 60º) (Eq. 1, where $a = 6.297 \cdot 10^{-7}$, $R^2 = 0.990$)

sampled for 30 seconds. Before the next measurement flow speed was let to stabilize after changing the flow.

D. Data treatment and accuracy estimation

All the proposed fits were evaluated using the coefficient of determination, R^2, as well as graphically. In addition, the observed data was compared to the predicted data and the mean absolute error was used as the measure of achieved accuracy.

III. Results and Discussion

A. Simulations

CFD simulations were used for testing multiple DPS distributions and body shapes, both of which have been established as key factors in the relation between pressure and velocity [7].

Using a symmetrical configuration with a semi-circular head shape, the relationship between the pressure difference on both sides of the prototype (ΔP_1 and ΔP_2) and the flow speed (V) shows a conic distribution (Fig. 3b). This relation between variables (Eq. 1) is explicit in the Pitot equation for 0º of angle of attack ($\Delta P_1 = \Delta P_2$) but also allows application for different angles with high precision ($R^2 = 0.99$).

$$V = \sqrt[4]{a\left(\Delta P_1^2 + \Delta P_2^2\right)} \qquad (1)$$

Where a is an empirical coefficient to be fitted according to the pressure sensor plugs distribution.

The Pitot relation has previously proposed for the calculous of velocity with APS [4], [5], [7], [21]. However, it has been usually applied to fish shape bodies which limits the usage of the relation independently of angle of attack.

Likewise, a in Eq. 1 depends solely on the pressure sensor distribution. For instance, if the pressure sensor ports are at 35º, a will be equal to $(2/\rho)^2$ where ρ is the density of water (1000 kg/m^3). This follows from the Pitot equation [9], the pressure distribution in spherical shapes where the hydrostatic pressure corresponds to the location of the head at 35º [22]. When increasing the angle above 35º, the pressure differential becomes negative which may be useful to increase the difference of pressure between ports in cases with low sensitivity sensors. In order to maximize this difference, the ports were angled at 60º in the prototype.

B. Data validation

Fig. 4 shows the raw data of the conducted experiments. When the prototype was facing the flow, same pressure distribution was observed in both sides (ΔP_1 and ΔP_2) (Fig. 4a). As the angle of attack increases, the pressure distribution changes accordingly. For instance, at ±30º the ports of one of the sensors were symmetrically distributed to the flow, thus, a pressure difference of 0 Pa was expected. Small deviances from 0 observed in Fig. 4a bottom left graph can be explained by the small errors in the orientation within the flow tunnel as well as in the port separation in the prototype head.

When the three variables involved (ΔP_1, ΔP_2 and V) are plotted together, similar distribution to one of the simulations can be observed (Fig. 4b). The fit ($R^2 = 0.96$, $a = 1.32 \cdot 10^{-6}$) is in accordance with previous remark, as the ports were situated above 35º, and the expected pressure drop between ports had to be higher than the theoretical one, thus a must be smaller than $(2/\rho)^2$ in order to calculate V.

It has also been observed that a slight increase in accuracy could be obtained if the degree of the root was also fitted ($R^2 = 0.98$). However, it rejects the original equation (Eq. 1). This increase may be explained by the introduced error during the prototype development or the manual change of the orientation in the flow tunnel.

In the Fig. 5a the relationship between actual and calculated velocity in the flow tunnel is presented. Test 1 was used for

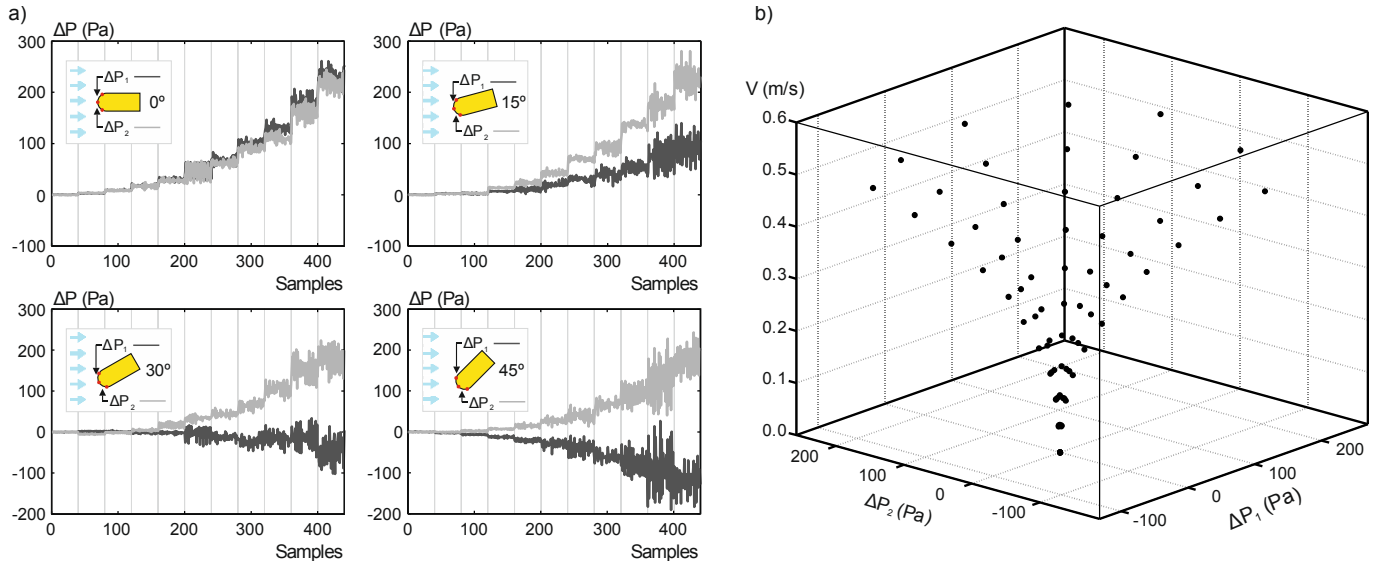

Figure 4. Summary of experimental results. a) Example of pressure distribution for each velocity (different steps of each graph) and for different angles of attack. For each velocity only one second of signal is shown downsampled to 40 Hz for a clear representation. b) Result of all studied scenarios in first run of experiments (Eq. 1, where $a = 1.32 \cdot 10^{-6}$, $R^2 = 0.9641$).

fitting the model and result of both tests has been plotted on the graph. It can be seen that the higher sensitivity of differential pressure sensors makes it possible to correctly estimate velocities < 0.15 m/s. The overall mean absolute error was 0.024 m/s (Fig. 5b), smaller than the one reported for APS with lower sensitivity (0.04 to 0.1 m/s [15]).

In order to obtain sufficient mean velocity measurements per second, the sampling frequency of the pressure has to be high. With the studied configuration, 0.15 Pa/bit sensitivity and 200 Hz sampling rate, a stable mean velocity calculation with sampling rates > 10 Hz can be achieved for the studied cases (Fig. 5b). It is worth mentioning that the original 200 Hz pressure signal can be converted directly into a 200 Hz velocity estimate. However, in absence of turbulence measurements it is not possible to validate it. Conventional DVLs provide a sampling rate of 1-5 Hz [3] which is lower than the one obtained, nevertheless DVL provides all vector components while the proposed system provides the mean magnitude.

We believe that further increasing in the pressure data acquisition rate can aid in increasing the sampling rate for the mean velocity. Likewise, the installation of sensors in vertical axis may provide, similarly to aircrafts, three vector components of the velocity.

IV. Summary and Conclusions

This paper demostrates the potential of DPS based systems for flow speed measurements. The use of DPS data in a reformulation of the Pitot relation proves to be applicable for different angles of attack. It is shown that the prototype and velocity equation provide highly accurate real-time flow speed calculations and, in contrast to APS, even for low velocities.

DPS requires lower ranges than APS to perform the same task, which in turn is translated in the possibility of reaching lower sensitivities. This is crucial for measuring low velocities or low velocity fluctuations. Likewise, the use of DPS reduces the necessary number of pressure sensors.

It was found that the tube and port locations and connections are vital to robust speedometry using DPS. Moreover, the use of a semi-circular head shape and fixed port separation provides near constant distributions of the pressure under a wide range of flow speeds.

V. Future Work

Future work will focus on the implementation of the sensing technology onto underwater vehicles. The fusion of DPS systems with typical AUV sensors such as inertial measurement units, could also lead to more reliable control paradigms for AUVs.

Acknowledgments

The research leading to these results has received funding from BONUS, the joint Baltic research and development programme, cofinanced by the European Union's Seventh Framework Programme (2007-2013) under the BONUS Implementation Agreement. National funding for this work has been provided by the Academy of Finland (under the grant 280715), the German Federal Ministry for Education and Research (BMBF FKZ:03F0687A), and the Estonian Environmental Investment Centre (KIK P.7254 C.3255). The work has also been partly financed by the EU FP7 project ROBOCADEMY (No. 608096) and by institutional research funding IUT (IUT33-9) of the Estonian Ministry of Education and Research.

References

[1] L. Stutters, H. Liu, C. Tiltman, and D. J. Brown, “Navigation technologies

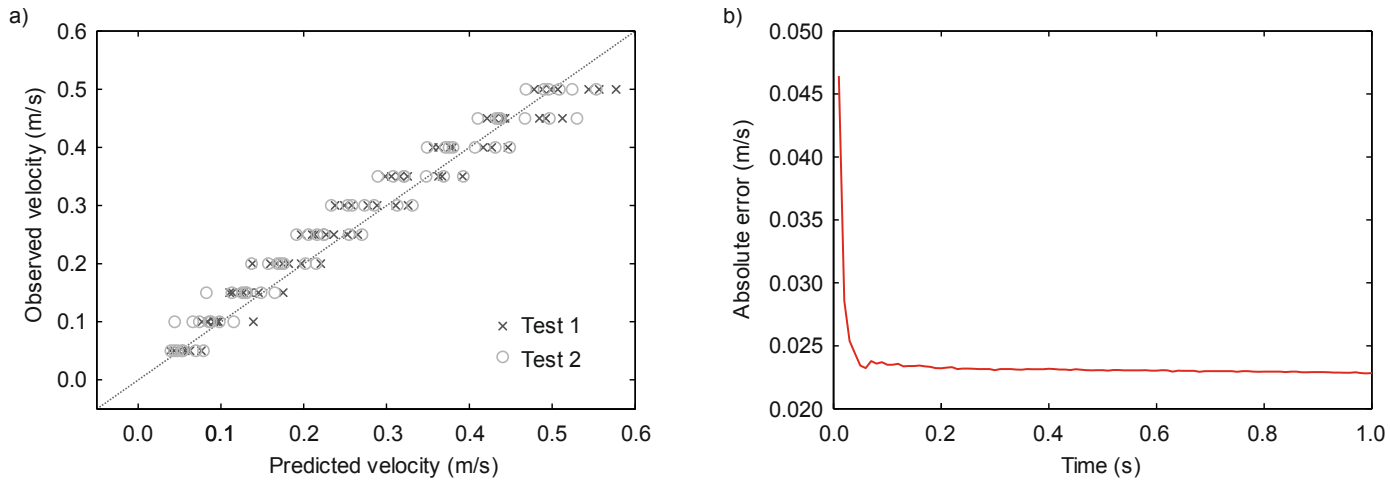

Figure 5. Summary of the velocity predictions. a) Observed velocity against predicted velocity for all test, Test 1 has been used for fitting of Eq. 1. b) Evolution of the mean absolute error as a function of increasing signal sampling duration.

for autonomous underwater vehicles," *IEEE Trans. Syst. Man, Cybern. Part C*, vol. 38, no. 4, pp. 581–589, 2008.

[2] M. J. Stanway, "Water profile navigation with an acoustic Doppler current profiler," in *OCEANS 2010 IEEE-Sydney*, 2010, pp. 1–5.

[3] J. C. Kinsey, R. M. Eustice, and L. L. Whitcomb, "A survey of underwater vehicle navigation: Recent advances and new challenges," in *IFAC CMCM*, 2006, pp. 1–12.

[4] T. Salumäe and M. Kruusmaa, "Flow-relative control of an underwater robot," *Proc. R. Soc. A Math. Phys. Eng. Sci.*, vol. 469, no. 2153, p. 20120671, 2013.

[5] W. Wang, Y. Li, X. Zhang, C. Wang, S. Chen, and G. Xie, "Speed Evaluation of a Freely Swimming Robotic Fish with an Artificial Lateral Line," in *IEEE ICRA*, 2016, pp. 1–6.

[6] D. L. Rudnick, R. E. Davis, C. C. Eriksen, D. M. Fratantoni, and M. J. Perry, "Underwater gliders for ocean research," *Mar. Technol. Soc. J.*, vol. 38, no. 2, pp. 73–84, 2004.

[7] J. F. Fuentes-Pérez, J. A. Tuhtan, R. Carbonell-Baeza, M. Musall, G. Toming, N. Muhammad, and M. Kruusmaa, "Current velocity estimation using a lateral line probe," *Ecol. Eng.*, vol. 85, pp. 296–300, 2015.

[8] C. Wang, W. Wang, and G. Xie, "Speed estimation for robotic fish using onboard artificial lateral line and inertial measurement unit," in *2015 IEEE ROBIO*, 2015, pp. 285–290.

[9] E. Ower and R. C. Pankhurst, *The measurement of air flow*. Elsevier, 2014.

[10] A. Cho, J. Kim, S. Lee, and C. Kee, "Wind estimation and airspeed calibration using a UAV with a single-antenna GPS receiver and pitot tube," *IEEE Trans. Aerosp. Electron. Syst.*, vol. 47, no. 1, pp. 109–117, 2011.

[11] E. N. Brown, C. A. Friehe, and D. H. Lenschow, "The use of pressure fluctuations on the nose of an aircraft for measuring air motion," *J. Clim. Appl. Meteorol.*, vol. 22, no. 1, pp. 171–180, 1983.

[12] J. Hacker and T. Crawford, "The BAT-probe: The ultimate tool to measure turbulence from any kind of aircraft (or sailplane)," *Tech. Soar.*, vol. 23, no. 2, pp. 43–46, 1999.

[13] K. H. Beij, "Aircraft Speed Instruments," 1933.

[14] K. E. Garman, K. A. Hill, P. Wyss, M. Carlsen, J. R. Zimmerman, B. H. Stirm, T. Q. Carney, R. Santini, and P. B. Shepson, "An Airborne and Wind Tunnel Evaluation of a Wind Turbulence Measurement System for Aircraft-Based Flux Measurements*," *J. Atmos. Ocean. Technol.*, vol. 23, no. 12, pp. 1696–1708, 2006.

[15] J. A. J. A. Tuhtan, J. F. J. F. Fuentes-Pérez, N. Strokina, G. Toming, M. Musall, M. Noack, J. K. K. Kämäräinen, M. Kruusmaa, and M. Kruusmaaa, "Design and application of a fish-shaped lateral line probe for flow measurement," *Rev. Sci. Instrum.*, vol. 045110, no. 4, pp. 1–8, 2016.

[16] C. J. Greenshields, *OpenFOAM: The open source CFD Toolbox*. OpenFOAM Foundation Ltd., 2015.

[17] M. H. Sangamesh, D. K. Ramesha, and S. Basu, "Transient simulation of flow past smooth circular cylinder at very high reynolds number using OpenFOAM.," *Appl. Mech. Mater.*, vol. 592–594, pp. 1972–1977, 2014.

[18] Honeywell, "TruStability® Board Mount Pressure Sensors-SSC Series." pp. 1–33, 2014.

[19] A. Industries, "Adafruit TCA9548A 1-to-8 I2C Multiplexer Breakout." pp. 1–20, 2015.

[20] Arduino, "https://www.arduino.cc/en/Main/ArduinoBoardMicro," 2016. .

[21] R. Venturelli, O. Akanyeti, F. Visentin, J. Ježov, L. D. Chambers, G. Toming, J. Brown, M. Kruusmaa, W. M. Megill, and P. Fiorini, "Hydrodynamic pressure sensing with an artificial lateral line in steady and unsteady flows," *Bioinspir. Biomim.*, vol. 7, no. 3, p. 36004, 2012.

[22] I. Paraschivoiu, *Subsonic Aerodynamics*. Presses inter Polytechnique, 2003.